Regular Article

PHYSICAL CHEMISTRY RESEARCH
Published by the
Iranian Chemical Society
www.physchemres.org
info@physchemres.org

Phys. Chem. Res., Vol. 7, No. 2, 271-293, June 2019
DOI: 10.22036/pcr.2019.153027.1551

Semi Empirical Calculation of Intermolecular Potentials and Transport Properties of Some Binary and Ternary Industrial Refrigerant Mixtures

D. Mohammad-Aghaie[a,*], E. Sookhaki[a] and F. Zargari[b]

[a]*Department of Chemistry, Shiraz University of Technology, Shiraz 71555-313, Iran*

[b]*Department of Chemistry, Computational Quantum Chemistry Laboratory, University of Sistan and Baluchestan, P. O. Box: 98135-674, Zahedan, Iran*

(Received 22 October 2018, Accepted 8 February 2019)

In this study, the intermolecular potential energies of some environment-friendly industrial HFC refrigerants were obtained through the inversion method based on the corresponding states principle. These potentials were later employed in calculation of transport properties (viscosity, diffusion, thermal conductivity and thermal diffusion factor) of some binary and ternary refrigerant mixtures, in the low density region. Predicted transport properties were compared with the available literature data leading to an acceptable agreement. The interaction potential was fitted to an analytical form, and the calculated low density transport properties were also fitted to the fairly exact equations. In the case of R410A and R421B mixtures, high density viscosity values were also calculated through the Vesovic-Wakeham method. Due to lack of experimental values on high density viscosities of these two mixtures, we could only compare the calculated high density viscosities for other available molar compositions of R124-R134a and R125-R32 binary mixtures with literature data, which an acceptable accordance was also observed.

Keywords: Transport properties, Intermolecular potential energy, Inversion method, Refrigerant mixtures

INTRODUCTION

Access to the reliable thermophysical properties of refrigerants and refrigerant mixtures is very important in design of industrial refrigeration equipment such as, air conditioning, refrigerators, heat pumps, power plants, refrigeration storage and small refrigeration compressors [1,2].

Generally, refrigerants are subdivided into the six main groups: (i) hydrocarbons (HC), (ii) hydrofluorocarbons (HFC), (iii) HFC/HC, (iv) hydrochlorofluorocarbons (HCFC), (v) carbon dioxide (R744), and (vi) ammonia (R717) [3]. This paper will focus on some binary and ternary HFC refrigerant mixtures, known for industrial applications, listed in Table 1.

These refrigerants with zero ODP (ozone depletion potential) and very low GWP (global warming potential), are considered as ozone-friendly refrigerants. Table 2 contains some physical properties for the more famous studied mixtures [4].

Although a database like REFPROP is a useful source in the open literature for different thermodynamic and transport properties of the refrigerants and refrigerant mixtures, yet the prediction methods based on the rigorous theories, have their own importance in the evaluation of transport properties of refrigerant mixtures [5].

The structure and properties of liquids, solids and gases are directly related to the intermolecular potential energy functions [6,7]. Fitting procedure [8] and inversion method are the two most common methods to determine the intermolecular potential energies from the experimental data. In the first approach, a potential function with certain number of adjustable parameters is assumed. The parameters are then optimized to achieve the reliable

*Corresponding author. E-mail: d_aghaie@sutech.ac.ir

Table 1. Studied Refrigerant Mixtures

Binary Mixture	Mole fractions of mixture constituents		
R410A	$x_{R32} = 0.6976$		$x_{R125} = 0.3024$
R507[A]	$x_{R125} = 0.4118$		$x_{R143a} = 0.5881$
R421B	$x_{R125} = 0.8281$		$x_{R134a} = 0.1718$
R423A	$x_{R134a} = 0.6481$		$x_{R227ea} = 0.3519$
Ternary mixture	Mole fractions of mixture constituents		
R404A	$x_{R125} = 0.3578$	$x_{R143a} = 0.6039$	$x_{R134a} = 0.03826$
R407C	$x_{R32} = 0.3811$	$x_{R125} = 0.1796$	$x_{R134a} = 0.4393$
R425A	$x_{R32} = 0.3211$	$x_{R134a} = 0.6151$	$x_{R227ea} = 0.06372$
R407E	$x_{R32} = 0.4026$	$x_{R125} = 0.1046$	$x_{R134a} = 0.4927$

Table 2. Physical Properties of Refrigerant Mixtures

Mixtures	R410A	R507[A]	R404A	R407C
Molecular weight (amu)	72.6	98.9	97.6	86.2
Critical temperature (°C)	70.17	70.8	72.14	86.05
Critical pressure (atm)	47.08	37.2	36.86	45.73
Boiling point at 1 atm (°C)	-51.6	-46.5	-46.6	-43.8
ODP	0.0	0.0	0.0	0.0
GWP(100 year)	2088	3300	3922	1774
Flammability[a]	A1	A1	A1	A1

[a]Flammability is the ability of a substance to burn due to fire or combustion, and materials can be classified based on the degree of flammability. In this classification, A1 means 100% noncombustible.

agreement with available experimental data. This technique fails to generate a unique potential function. On the other hand, the inversion method of Smith *et al.* [9,10] produces a spherical pair potential energy, with no need of any supplied model potential [7,11].

It is more common to use the viscosity data to obtain the potential energy function, through the inversion method. This is based on two reasons: viscosity is the most accurate property among transport properties of the system, and its measurement is experimentally more practical than other transport properties [12,13]. In continuation of our previous works on the calculation of potential energy functions and transport properties of different mixtures [12-15], our main purpose is using the inversion method, in order to determine the accurate pair potential energy functions of some alternative refrigerant mixtures (mentioned above), from

corresponding states correlation of viscosity. The inverted potential energy functions are then fitted into an analytical potential model and are also employed to predict low density viscosity, diffusion and thermal diffusion factor of studied refrigerant mixtures, at wide temperature range, using the Chapman-Enskog version of the kinetic theory [16]. Thermal conductivity is also predicted by the Schreiber *et al.'s* [17] method. High-density viscosity values for 2 refrigerant systems, including R410A, and R421B are calculated through the Vesovic-Wakeham method [18,19]. The overall results demonstrate an acceptable agreement between the calculated and literature data on transport properties, both in the low and high density regions.

CALCULATION OF TRANSPORT PROPERTIES OF GASES AT ZERO DENSITY REGIME

Once the interaction potential is determined, transport properties are predictable from the Chapman-Enskog expressions [16,20] through solving the Boltzmann kinetic equation, at low density. Transport coefficients of gases can be expressed in terms of collision integrals, namely $\Omega^{(l,s)}(T)$, which are the binary interaction parameters. The superscripts l and s denote weighting factors that account for the transport mechanism by molecular collision.

Collision integrals, $\Omega^{(l,s)}$ are related to intermolecular forces and calculated from the following three-fold integration:

$$\theta = \pi - 2b\int_{r_m}^{\infty} \frac{r^{-2}dr}{\left\{1-\left(\frac{b^2}{r^2}\right)-\left[\frac{2V(r)}{m\omega^2}\right]\right\}^{1/2}} \tag{1}$$

$$Q^{(1)}(E) = 2\pi\left[1-\frac{1+(-1)^l}{2(1+l)}\right]^{-1}\int_0^{\infty}(1-\cos^l\theta)bdb \tag{2}$$

$$\Omega^{(l,s)}(T) = \left[(s+1)!\,(k_BT)^{s+2}\right]^{-1}\int_0^{\infty}(Q^{(1)}(E)\times e^{\left(-\frac{E}{k_BT}\right)})E^{s+1}dE \tag{3}$$

where θ is the scattering angle; $Q^{(1)}(E)$, the transport collision integral; b, the impact parameter; E, the relative kinetic energy of colliding partners; r, the interparticle distance; r_m, the closest approach of two molecules; ω, the relative velocity of colliding molecules, and k_BT, the molecular thermal energy.

After determination of the intermolecular potential [$V(r)$] by the inversion method (as discussed later), it serves as an input in Eq. (1) to yield the scattering angle (θ). This quantity enters the second equation and gives rise to the transport cross section, which provides the required information to compute the collision integrals, *via* Eq. (3).

Calculation of transport properties is done more easily by the definition of collision integrals as dimensionless reduced quantities. Reduced collision integral is defined as:

$$\Omega^{*(l,s)} = \frac{\Omega^{(l,s)}}{\pi\sigma^2} \tag{4}$$

where the σ parameter is the intermolecular separation, such that $V(\sigma) = 0$. Numerical differentiation, along with the recursion relationship, generates higher order collision integrals [21].

$$\Omega^{*(l,s+1)} = \Omega^{*(l,s)}\left[1+\frac{1}{s+2}\frac{d\ln\Omega^{*(l,s)}}{d\ln T^*}\right] \tag{5}$$

Reduced temperature (T^*) is defined as:

$$T^* = \frac{k_B}{\varepsilon} \tag{6}$$

where ε is the well depth of intermolecular potential. For the sake of calculation convenience, in higher approximations of transport properties, the following recurring ratios of collision integrals are employed [21].

$$A^* = \Omega^{*(2,2)}/\Omega^{*(1,1)} \tag{7}$$

$$B^* = [5\Omega^{*(1,2)} - 4\Omega^{*(1,3)}]/\Omega^{*(1,1)} \tag{8}$$

$$C^* = \Omega^{*(1,2)}/\Omega^{*(1,1)} \tag{9}$$

$$E^* = \Omega^{*(2,3)}/\Omega^{*(2,2)} \tag{10}$$

$$F^* = \Omega^{*(3,3)}/\Omega^{*(1,1)} \tag{11}$$

The value of each of these ratios is approximately unity, and exactly unity for the rigid spheres. Low density viscosities (η), diffusion (D) and thermal diffusion coefficients (α) are calculated based on the Chapman-Enskog theory [16,20], through Eqs. ((12)-(25)), reported in ref. [14].

In the basic development of Chapman-Enskog theory, internal degrees of freedom and inelastic collision between molecules are not taken into account, so this theory cannot be employed for the prediction of thermal conductivities.

In this study, in order to calculate the thermal conductivities of refrigerant mixtures, the Schreiber *et al.'s* method [17] for polyatomic dilute gas mixtures was employed. Schreiber *et al.* [17] have introduced a new expression for the thermal conductivity of N-component polyatomic gas mixture in the dilute gas limit, based on the Thijsse approximation [22].

They derived the L_{ij} elements, in terms of measurable quantities, rather than effective cross-sections. The resulting thermal conductivity expressions (Eqs. (12)-(16)) were analogous with, and no more complicated than the corresponding relationships for purely monatomic mixtures.

$$\lambda = \frac{\begin{vmatrix} L_{11} & L_{12} & \cdots & L_{1\nu} & x_1 \\ L_{21} & L_{22} & \cdots & L_{2\nu} & x_2 \\ \vdots & \vdots & \ddots & \vdots & \vdots \\ L_{\nu 1} & L_{\nu 1} & \cdots & L_{\nu\nu} & x_\nu \\ x_1 & x_2 & \cdots & x_\nu & 0 \end{vmatrix}}{\begin{vmatrix} L_{11} & L_{12} & \cdots & L_{1\nu} \\ L_{21} & L_{22} & \cdots & L_{2\nu} \\ \vdots & \vdots & \ddots & \vdots \\ L_{\nu 1} & L_{\nu 1} & \cdots & L_{\nu\nu} \end{vmatrix}} \tag{12}$$

In the above equation x_i is the mole fraction of species i, and the symbol λ indicates the full formal first order kinetic theory result, obtained by means of expansion in Thijsse basis vectors [22]. Thijsse approximation considers the total energy as the dominant factor in determination of thermal conductivity.

The relevant determinant elements, L_{ij} are given by [21]:

$$L_{qq} = \frac{x_q^2}{\lambda_q} + \sum_{\mu \neq q}^{\nu} \frac{25 x_q x_\mu}{8 A^*_{q\mu} \lambda_{q\mu}} \left(\frac{R}{C^0_{pq}}\right)^2 \left[\frac{25}{4} y_\mu^4 + \frac{15}{2} y_q^4 - 3 y_\mu^4 B^*_{q\mu} + 4 y_q^2 y_\mu^2 A^*_{q\mu} + \left(\frac{C^0_{pq}}{R} - 2.5\right)\right] \tag{13}$$

and

$$L_{qq'} = -\frac{25 x_q x_{q'} y_q^2 y_{q'}^2}{8 A^*_{qq'} \lambda_{qq'}} \left(\frac{R}{C^0_{pq}}\right)\left(\frac{R}{C^0_{pq'}}\right)\left[\frac{55}{4} - 3B^*_{qq'} - 4A^*_{qq'}\right] \tag{14}$$

where λ_q is the thermal conductivity of pure molecular species q; λ_{qq}, the interaction thermal conductivity; $C_{pq}{}^0$, the ideal gas isobaric heat capacity of q; R, the gas constant, and quantities A^* and B^* are ratios of effective cross-sections given by Eqs. (7) and (8), respectively. In addition, y_q is the mass ratio of species q, given by:

$$y_q^2 = \frac{M_q}{\left(M_q + M_{q'}\right)} \tag{15}$$

where M_q is the molecular weight of species q. The interaction thermal conductivity is related to the more readily available, interaction viscosity, $\eta_{qq'}$, through the following equation:

$$\lambda_{qq'} = \frac{15}{8} R \frac{\left(M_q + M_{q'}\right)}{M_q M_{q'}} \eta_{qq'} \tag{16}$$

Evaluation of thermal conductivity for a multicomponent polyatomic gas mixture requires a knowledge of thermal conductivity and isobaric heat capacity of each of the pure species. This information is readily available for a large number of fluids as a function of temperature, either in terms of correlations or directly from experimental information. Furthermore, three binary interaction parameters, namely, $\eta_{qq'}$, A^*, and B^*, as functions of temperature, are also required. In the present work, these quantities were obtained from the calculated interaction viscosity and collision integral ratios, provided by the inversion method.

VISCOSITY AT HIGH DENSITY REGION

According to the Di Pippo *et al.'s* method, viscosity of a dense gas mixture, containing N components can be written in the form [23]:

$$\eta(\rho,T)=-\frac{\begin{vmatrix} H_{11} & H_{12} & \cdots & H_{1N} & x_1 \\ H_{21} & H_{22} & \cdots & H_{2N} & x_2 \\ \vdots & \vdots & \ddots & \vdots & \vdots \\ H_{N1} & H_{N2} & \cdots & H_{NN} & x_N \\ x_1 & x_2 & \cdots & x_N & 0 \end{vmatrix}}{\begin{vmatrix} H_{11} & H_{12} & \cdots & H_{1N} \\ H_{21} & H_{22} & \cdots & H_{2N} \\ \vdots & \vdots & \ddots & \vdots \\ H_{N1} & H_{N2} & \cdots & H_{NN} \end{vmatrix}}+\kappa_{mix} \tag{17}$$

$$Y_i = x_i\left[1+\sum_{j=1}^{N}\frac{m_i}{m_i+m_j}x_j\alpha_{ij}\overline{X}_{ij}\rho\right] \tag{18}$$

$$H_{ii}=\frac{x_i^2\overline{X}_{ii}}{\eta_i}+\sum_{j=1}^{N}\frac{x_ix_j\overline{X}_{ij}}{2\eta_{ij}^{0}A_{ij}^{*}}\frac{m_im_j}{(m_i+m_j)^2}\left[\frac{20}{3}+\frac{4m_j}{m_i}A_{ij}^{*}\right] \tag{19}$$

$$H_{ij}(i\neq j)=-\frac{x_ix_j\overline{X}_{ij}}{2A_{ij}^{*}\eta_{ij}^{0}}\frac{m_im_j}{(m_i+m_j)^2}\left[\frac{20}{3}-4A_{ij}^{*}\right] \tag{20}$$

$$\kappa_{mix}=(\frac{16}{5\pi})\frac{15}{16}\rho^2\sum_{j=1}^{N}\sum_{i=1}^{N}x_ix_j\overline{X}_{ij}\alpha_{ij}^2\eta_{ij}^{0} \tag{21}$$

where ρ is the molar density, x_i and x_j are mole fractions of species i and j, and m_i and m_j are their respective molecular masses. A^* is a weak functional of intermolecular potential for i - j interactions and is readily available using the corresponding-states principle [24]. The symbol η_i^0 represents the viscosity of pure component i in the dilute-gas limit, while η_{ij}^0 represents the interaction viscosity for species i - j in the same conditions. The parameter α_{ij} is a volume accounting for the mean free-path shortening in the dense gas that is related to the covolume of the pair of molecules i and j, whereas $\overline{X}_{ij}$ is the pseudoradial distribution function for the hard spherical molecules i and j, in the presence of all other species in the mixture. In order to implement the above procedure for evaluation of mixture viscosity values, the pseudoradial distribution function for pure gases are required. A pseudo-radial distribution function, $\overline{X}_i$, is identified for each real pure component at a particular temperature and the density of interest, from measurements of the pure component viscosity of each fluid. This can be accomplished by writing Eq. (17), for a pure fluid and solving for the pseudo-radial distribution function at each density [18,24]. Hence,

$$\overline{X}_i(\rho,T)=\frac{B_\eta}{2}\frac{\left(\eta_i-\rho\alpha_{ii}\eta_i^{(0)}\right)}{\rho^2\alpha_{ii}^2\eta_i^{(0)}}\pm\beta_\eta\left[\left(\frac{\eta_i-\rho\alpha_{ii}\eta_i^{(0)}}{2\rho^2\alpha_{ii}^2\eta_i^{(0)}}\right)^2-\frac{1}{\beta_\eta\rho^2\alpha_{ii}^2}\right]^{1/2} \tag{22}$$

where,

$$\frac{1}{\beta_\eta}=\frac{1}{4}+\left(\frac{16}{5\pi}\right)\frac{15}{16}=1.2049 \tag{23}$$

and η_i is the pure-component viscosity at the molar density ρ and temperature T, at which the mixture properties are required. In general, there are two possible solutions for Eq. (22), $\overline{X}_i^+$ and, $\overline{X}_i^-$ corresponding to the positive and negative signs of this equation. Vesovic and Wakeham [18,19] adopted the Sandler and Fiszdon method [25] in handling of these two solutions. According to their method, although both solutions for $\overline{X}_i$ will reproduce the pure component viscosity, only one of the solutions is physically plausible at a given density.

At low density, the physically plausible $\overline{X}_i$ should be smooth and monotonically decreasing to $\overline{X}_i=1$, as ρ tends to zero; while at high densities, the pseudo-radial distribution function, $\overline{X}_i$, should increase monotonically. To ensure this behavior, it is necessary to switch from one branch, $\overline{X}_i^-$, valid for low densities, to the other branch of the solution, $\overline{X}_i^+$, at a particular density, ρ^*, where the two roots are equal, so that [26]:

$$\overline{X}_i^+(\rho^*,T)=\overline{X}_i^-(\rho^*,T) \tag{24}$$

These equalities for different densities lead to the result that:

$$\left(\frac{\eta_i}{\eta_i^{(0)}\alpha_{ii}\rho}\right)_{\min} = \frac{\eta_i}{\eta_i^{(0)}\alpha_{ii}\rho^*} = \left(\frac{2}{\sqrt{\beta_\eta}}+1\right) = 3.1954 \tag{25}$$

The group $\left(\frac{\eta_i}{\eta_i^{(0)}\rho}\right)$ as a function of density displays its minimum value at the density ρ^*. Thus, from experimental, or correlated, values of $\eta_i(\rho,T)$, by plotting $\left(\frac{\eta_i}{\eta_i^{(0)}\rho}\right)$ as a function of ρ for each temperature, it is possible to locate the density of the minimum, ρ^*(T), and to determine the value of the corresponding group at the minimum. Subsequently, application of Eq. (25) yields a value of α_{ij}. In this way, we can make sure that values of $\overline{X}_i$ will be entirely real and that the transition between the two roots is accomplished smoothly.

In practice, the procedure is implemented by establishing the density for which:

$$\left(\frac{d\eta_i}{d\rho}\right)_T = \frac{\eta_i}{\rho} \tag{26}$$

In order to calculate mixture properties, one needs to construct the pseudoradial distribution function $\overline{X}_{ij}$ for species i and j in the mixture. This is achieved by implementing the mixing rule, first developed in Ref. [27]. The functions $\overline{X}_{ij}$ for all possible values of i and j are obtained from the following equation:

$$\overline{X}_{ij}(\rho,T) = 1+\frac{2}{5}\sum_{k=1}^{N} x_k\left(\overline{X}_k-1\right)+\frac{\left\{\frac{6}{5}\left(\overline{X}_i-1\right)^{1/3}\left(\overline{X}_j-1\right)^{1/3}\sum_{k=1}^{N} x_k\left(\overline{X}_k-1\right)^{2/3}\right\}}{\left(\overline{X}_i-1\right)^{1/3}+\left(\overline{X}_j-1\right)^{1/3}} \tag{27}$$

The α_{ij} parameters are also obtained from a rigid-sphere mixing rule:

$$\alpha_{ij} = \frac{1}{8}\left(\alpha_{ii}^{1/3}+\alpha_{jj}^{1/3}\right)^3 \tag{28}$$

INVERSION PROCEDURE

The inversion method based on the viscosity collision integrals uses the principle of corresponding states for generating the intermolecular potentials from the bulk properties [28].

The most important advantage of inversion method is that the values of one accurately known property, such as viscosity, can be used to predict other properties, which are known less accurately from the experiment.

The inversion technique is initiated by an estimation of G_η (the inversion function) from an initial intermolecular potential energy. Lennard-Jones potential is one of the most popular interaction potential models that can be used for calculation of the thermophysical properties of monatomic or spherical fluids. It should be mentioned that the inversion function depends on the reduced temperature (T^*).

Therefore, it is possible to transform a set of reduced viscosity collision integrals, $\Omega^{*(2,2)}$ (over wide range of reduced temperatures) and the estimation of G_η function from initial model potential (LJ 12-6) to a pair of (V/ε, r/σ) data on the potential energy curve, through Eqs. ((28) and (29)).

$$\frac{V}{\varepsilon} = V^* = G_\eta(T^*)T^* \tag{28}$$

$$\frac{r}{\sigma} = r^* = (\Omega^{*(2,2)})^{1/2} \tag{29}$$

The Gatland version [29] of the computer program developed by O'Hara and Smith [30,31] solves three consecutive integral Eqs. ((1)-(3)) that transforms the new potentials to the improved collision integrals. This process is repeated until convergence between calculated and experimental collision integrals occurs.

In order to develop an iterative scheme, it is necessary to extrapolate potential $V(r)$, to both larger and smaller intermolecular separations than the experimental range. At long range, this extrapolation is performed by means of an inverse sixth-power function:

$$V(r) = C_6 r^{-6} \tag{30}$$

and at short range by means of an inverse 12th function:

$$V(r) = Ar^{12} \tag{31}$$

Table 3. The Reduced Collision Integrals and their Ratios for the HFC-refrigerant Mixtures

$\log T^*$	$\Omega^{*(1,1)}$	$\Omega^{*(2,2)}$	A^*	B^*	C^*	E^*	F^*
-1	4.1422	4.2772	1.0326	1.2256	0.8672	0.9057	0.9203
-0.9	3.7762	3.9202	1.0381	1.2194	0.8653	0.9055	0.9203
-0.8	3.4396	3.5969	1.0457	1.2233	0.8642	0.9077	0.9200
-0.7	3.1290	3.3078	1.0571	1.2404	0.8612	0.9099	0.9180
-0.6	2.8369	3.0434	1.0728	1.2653	0.8545	0.9082	0.9143
-0.5	2.5570	2.7882	1.0903	1.2861	0.8444	0.9005	0.9104
-0.4	2.2878	2.5304	1.1060	1.2927	0.8336	0.8883	0.9074
-0.3	2.0334	2.2694	1.1161	1.2816	0.8257	0.8755	0.9060
-0.2	1.8005	2.0146	1.1189	1.2555	0.8233	0.8668	0.9064
-0.1	1.5954	1.7795	1.115	1.2221	0.8277	0.8650	0.9092
0	1.4212	1.5747	1.1081	1.1875	0.8383	0.8707	0.9147
0.1	1.2773	1.4051	1.1001	1.1571	0.8534	0.8826	0.9231
0.2	1.1610	1.2698	1.0936	1.1336	0.8704	0.8977	0.9337
0.3	1.0679	1.1642	1.0901	1.1165	0.8874	0.9135	0.9459
0.4	0.9933	1.0822	1.0895	1.10551	0.9026	0.9276	0.9584
0.5	0.9328	1.0180	1.0912	1.0986	0.9153	0.9389	0.970
0.6	0.8831	0.9663	1.0942	1.0942	0.9254	0.9474	0.9810
0.7	0.8411	0.9232	1.0977	1.0914	0.9331	0.9531	0.9901
0.8	0.8047	0.8859	1.1009	1.0891	0.9389	0.9570	0.9975
0.9	0.7727	0.8527	1.1035	1.0869	0.9433	0.9596	1.0034
1	0.7440	0.8223	1.1053	1.0848	0.9467	0.9615	1.0080
1.1	0.7178	0.7942	1.1064	1.0829	0.9495	0.9629	1.0114
1.2	0.6937	0.7681	1.1072	1.0820	0.9516	0.9643	1.0137
1.3	0.6713	0.7438	1.1080	1.0824	0.9530	0.9656	1.015
1.4	0.6501	0.7208	1.1089	1.0831	0.9539	0.9661	1.0165
1.5	0.6298	0.6984	1.1089	1.0815	0.9545	0.9649	1.0186
1.6	0.6105	0.6755	1.1063	1.0751	0.9557	0.9624	1.0215
1.7	0.5926	0.6518	1.0999	1.0633	0.9582	0.9602	1.0243
1.8	0.5765	0.6281	1.0893	1.0480	0.9626	0.9596	1.0259
1.9	0.5629	0.6055	1.0756	1.0325	0.9684	0.9613	1.0255
2	0.5521	0.5854	1.0603	1.0189	0.9750	0.9655	1.0232

Table 4. Calculated Parameters: Sum of Standard Errors (SSE), Correlation Coefficients (R) and Root Mean Square Error (RMSE) of Tosi/Fumi Potential (Eq. (32)) for some of the Binary HFC-refrigerant Gas Mixtures

Coefficient	Mixture			
	R410A	R507[A]	R421B	R423A
(ε/k) (K)	272.5133109	288.4875621	258.3516015	321.2980372
σ (Å)	4.64	5.0725	5.17	5.24
A	0.02407	0.01485	0.02272	0.02827
ρ	0.3408	0.3652	0.3796	0.3848
C	2466	3966	4473	6031
D	1193	2207	2688	3723
SSE	1.626×10^7	1.822×10^7	1.462×10^7	2.261×10^7
R-square	0.9967	0.9967	0.9967	0.9967
RMSE	645.7	683.6	612.2	761.3

where *V(r)* is the intermolecular pair potential function, *r* the intermolecular separation, C_6 the dispersion coefficient and *A* is a constant. Therefore, the effective potential energies obtained from the inversion method were used to evaluate the improved kinetic theory collision integrals, over the given range. Generally, calculations of other properties are considerably facilitated by the existence of numerical tables of collision integrals and their ratios calculated using Eqs. ((7)-(11)), and reported in Table 3.

The inverted potential energy values of HFC-refrigerant gas mixtures were fitted to the Born-Mayer-Huggins or Tosi/Fumi analytical potential model [32,33]:

$$V = A\exp(\frac{\sigma - r}{\rho}) - \frac{C}{r^6} + \frac{D}{r^8} \quad r < r_C \tag{32}$$

The fitting procedure was performed for all studied binary gas mixtures, where Table 4 contains the resulting parameter values such as: sum of standard errors (SSE= $\sum (Y_i - \hat{Y}_i)^2$) and root-mean-square errors (RMSE= $\sqrt{\frac{\sum_{i=1}^{n} (X_{cal,i} - X_{\mathrm{mod}\,el,i})^2}{n}}$). RMSE shows the difference between the predicted values of Tosi/Fumi model and the calculated values of the system. The last parameter is correlation coefficient (R), which varies between +1 and -1, where +1 represents accurate correlation between model and data for each fitting.

RESULTS AND DISCUSSION

Precise assessment of any potential energy is confirmed by its ability to reproduce thermophysical properties with the acceptable accuracies. In this respect, transport properties of 4 binary and 4 ternary refrigerant gas mixtures were estimated from the present model potential energies. Tables 5-8 contain the predicted binary gas mixture viscosities, diffusion coefficients, and thermal diffusion factors at low density in the temperature range 200 K < T < 973.15 K, through the Chapman-Enskog theory (Eqs. (12)-(25) in ref. [14]). In addition, thermal conductivities of

Table 5. Predicted Transport Properties of R410A Binary Mixture

T (K)	$10^6\eta$ (Pa s)	10^4D_{12} ($m^2\ s^{-1}$)	αT	$10^3\lambda$ ($W\ mK^{-1}$)
200	8.514	0.0243	-0.0165	-
250	10.726	0.0380	0.0016	10.888
273.15	11.189	0.0456	0.0115	12.048
293.15	12.599	0.0522	0.0212	13.644
300	12.897	0.0545	0.0245	14.136
313.15	13.475	0.0593	0.0310	15.130
333.15	14.322	0.0672	0.0405	16.680
353.15	15.156	0.0752	0.0497	18.391
373.15	15.978	0.0835	0.0586	20.154
423.15	18.002	0.1065	0.0805	24.966
473.15	19.917	0.1310	0.0990	-
523.15	21.777	0.1583	0.0993	-
573.15	23.538	0.1872	0.1309	-
623.15	25.266	0.2178	0.1440	-
673.15	26.908	0.2512	0.1560	-
723.15	28.474	0.2853	0.1654	-
773.15	30.020	0.3211	0.1742	-
873.15	32.954	0.3992	0.1896	-
973.15	35.722	0.4815	0.2006	-

aforementioned gas mixtures were computed *via* expressions 12-16, in a limited temperature range, where both mixture components are in the gas phase [34].

It should be mentioned that in order to calculate mixture transport properties, we need to know binary potential parameters, σ_{12} and ε_{12}. We took the scaling parameters σ and ε for R134a from ref [35]. For the remaining four refrigerants (R125, R32, R143a and R227ea), the σ values were calculated through the following equation [36],

$$\sigma = 0.809(V_C)^{1/3} \quad (33)$$

where V_C is the critical volume. The ε values were evaluated from the corresponding states correlation for $\Omega^{*(2,2)}$, given in ref. [37], in conjunction with a nonlinear least-squares method. Binary potential parameters (σ_{12} and ε_{12}) were calculated using the famous combining rule, known as Lorentz-Berthelot rule (Eqs. (34), (35)).

Table 6. Predicted Transport Properties of R507[A] Binary Mixture

T (K)	$10^6\eta$ (Pa s)	$10^4 D_{12}$ ($m^2\ s^{-1}$)	αT	$10^3\lambda$ ($W\ mK^{-1}$)
200	7.907	0.0175	-0.0074	-
250	9.953	0.0274	-0.0017	10.827
273.15	10.914	0.0328	0.0020	12.503
293.15	11.751	0.0379	0.0052	14.050
300	12.014	0.0396	0.0065	14.585
313.15	12.518	0.0430	0.0089	15.634
333.15	13.313	0.0485	0.0125	17.304
353.15	14.146	0.0545	0.0162	19.063
373.15	14.921	0.0607	0.0196	20.842
423.15	16.776	0.0771	0.0281	25.448
473.15	18.636	0.0955	0.0360	-
523.15	20.341	0.1150	0.0429	-
573.15	22.101	0.1368	0.0497	-
623.15	23.654	0.1590	0.0548	-
673.15	25.220	0.1829	0.0599	-
723.15	26.795	0.2089	0.0648	-
773.15	28.195	0.2349	0.0682	-
873.15	31.007	0.2917	0.0751	-
973.15	33.622	0.3528	0.0802	-

$$\sigma_{12} = (\sigma_1 + \sigma_2)/2 \quad (34)$$

$$\varepsilon_{12} = (\varepsilon_1 \varepsilon_2)^{1/2} \quad (35)$$

Predicted viscosity, diffusion coefficients, and thermal diffusion factors for the four studied binary mixtures were correlated respectively with Eqs. ((36)-(38)) [13], using the MATLAB program, in the 200 K < T < 973.15 K temperature range.

$$\ln\left(\frac{\eta}{\eta_0}\right) = a_\eta \ln\left(\frac{T}{T_0}\right) + \frac{b_\eta}{T} + \frac{c_\eta}{T} + d_\eta \quad (36)$$

where η_0 = 1 μPa s and T_0 = 1 K.

$$\ln\left(\frac{PD}{P_0 D_0}\right) = a_D \ln\frac{T}{T_0} + \frac{b_D}{T} + C_D \quad (37)$$

where P_0 = 1 atm, and D_0 = 1 $cm^2\ s^{-1}$.

Table 7. Predicted Transport Properties of R421B Binary Mixture

T (K)	$10^6\eta$ (Pa s)	10^4D_{12} ($m^2\ s^{-1}$)	α_T	$10^3\lambda$ ($W\ mK^{-1}$)
200	8.514	0.0163	-0.0024	-
250	10.704	0.0255	0.0013	10.644
273.15	11.685	0.0304	0.0033	12.260
293.15	12.563	0.0349	0.0050	13.729
300	12.854	0.0365	0.0056	14.240
313.15	13.379	0.0398	0.0068	15.212
333.15	14.183	0.0450	0.0086	16.736
353.15	14.986	0.0502	0.0102	18.301
373.15	15.816	0.0557	0.0118	19.902
423.15	17.670	0.0710	0.0158	24.024
473.15	19.529	0.0873	0.0189	-
523.15	21.218	0.1055	0.0223	-
573.15	22.881	0.1242	0.0246	-
623.15	24.468	0.1448	0.0270	-
673.15	25.974	0.1664	0.0291	-
723.15	27.465	0.1888	0.0306	-
773.15	28.892	0.2128	0.0322	-
873.15	31.585	0.2635	0.0348	-
973.15	34.182	0.3183	0.0367	-

$$\ln \alpha^{-1}{}_T = \frac{a_\alpha}{T^*} + \frac{b_\alpha}{T^{*2}} + c_\alpha \ln T^* + d_\alpha (\ln T^*)^2 + \frac{e_\alpha}{\ln T^*} + \frac{f_\alpha}{(\ln T^*)^2} \quad (38)$$

The mixture thermal conductivities, λ_{12} are presented with the following fourth-order polynomial function [13] which is valid in the temperature range 250 K < T < 423.15 K for R410A, R507 [A], R421B and the temperature range 273.15 K < T < 423.15 K for R423A.

$$\lambda = a_\lambda + b_\lambda T + c_\lambda T^2 + d_\lambda T^3 + e_\lambda T^4 \quad (39)$$

All above parameters are given in Table 9 for the binary studied mixtures. SSE, R^2 and RMSE, the indicators of fit quality, are also included in this table.

In addition, Table 10 contains the viscosity and thermal conductivity values of some ternary refrigerant mixtures. In order to assess the reliability of inverted potential energy functions and calculated transport properties, these

Table 8. Predicted Transport Properties of R423A Binary Mixture

T (K)	$10^6\eta$ (Pa s)	10^4D_{12} (m^2 s^{-1})	α_T	$10^3\lambda$ (W mK^{-1})
200	7.798	0.0132	-0.0139	-
250	9.820	0.0207	-0.0085	-
273.15	10.759	0.0247	-0.0039	11.749
293.15	11.571	0.0284	-0.0006	13.184
300	11.841	0.0298	0.0022	13.645
313.15	12.374	0.0326	0.0051	14.661
333.15	13.171	0.0368	0.0098	16.173
353.15	13.970	0.0412	0.0151	17.711
373.15	14.740	0.0459	0.0201	19.211
423.15	16.648	0.0587	0.0321	23.132
473.15	18.487	0.0727	0.0434	-
523.15	20.267	0.0882	0.0537	-
573.15	21.984	0.1043	0.0627	-
623.15	23.615	0.1222	0.071	-
673.15	25.199	0.1408	0.0781	-
723.15	26.747	0.1602	0.0843	-
773.15	28.211	0.1811	0.0902	-
873.15	31.050	0.2252	0.0996	-
973.15	33.722	0.2732	0.1073	-

quantities were compared with the literature data. Figure 1 shows the deviations of calculated viscosities of two binary and three ternary refrigerant mixtures from the experimental values [38,39]. Binary mixtures are R410A and R507[A] that their experimental viscosity values have been measured using an oscillating-disk viscometer over the temperature range 298.98 K-397.39 K [38]. Average absolute deviation (AAD) values of the calculated binary viscosity coefficients for R410A and R507[A] were estimated to be 0.767% and 2.138%, respectively. Deviations of the calculated viscosity values of three studied ternary refrigerant mixtures are as follows: R404A shows AAD% = 1.967 at temperature range 305.5 K-392.59 K [38], R407C gives rise to AAD% = 1.124 at temperature range 298.15 K-423.15 K and finally R407E shows AAD% = 0.848 at the temperature range of 298.15 K-423.15 K [39].

Figure 2 shows the deviations of calculated viscosity values, for the two binary refrigerant mixtures, R125-R134a [40] and R125-R32 [41], over the temperature range 298.15 K-423.15 K, from literature data at three different

Table 9. The Nonlinear Least-squares Parameters, Sum of Standard Errors (SSE), Correlation Coefficients (R) and Root Mean Square Errors (RMSE) for Eqs. (36)-(39)

Coefficients of Eq. (36)							
Mixture	a_η	b_η	c_η	d_η	R^2	SSE	RMSE
R-410A	3.407	-375.9	39.14	-4.13	0.9737	0.0834	0.07719
R-507[A]	-2.874	-377.8	130.6	-9.273	0.9738	0.0835	0.07725
R421B	-2.663	-360.5	56.64	-9.481	0.9759	0.0700	0.07073
R423A	-1.733	-382.9	152.8	-9.128	0.9729	0.089	0.07973

Coefficients of Eq. (37)						
	a_D	b_D	c_D	R^2	SSE	RMSE
R-410A	1.232	-773.3	-7.05	0.9645	0.4809	0.179
R-507[A]	0.6439	-777.6	-0.111	0.9645	0.4871	0.1802
R421B	-0.8689	-768.3	-1.732	0.9645	0.4755	0.178
R423A	-0.3349	-748	-1.145	0.9615	0.5383	0.1894

Coefficients of Eq. (38)									
	a_α	b_α	c_α	d_α	e_α	f_α	R^2	SSE	RMSE
R-410A	-5.601	7.581	0.9499	0.02653	0.508	0.4553	0.9563	1.141	0.3221
R-507[A]	0.351	3.866	-0.1014	0.4706	0.9412	0.2038	0.9781	0.4218	0.2054
R421B	-1.946	4.531	0.8557	0.5665	0.9233	0.674	0.992	0.121	0.1049
R423A	-8.105	9.332	0.5449	0.8322	0.8321	1.182	0.957	1.475	0.4048

Coefficients of Eq. (39)								
	a_λ	b_λ	c_λ	d_λ	e_λ	R^2	SSE	RMSE
R-410A	151.3	-1.77	0.00796	-1.53×10^{-5}	1.11×10^{-8}	0.9996	0.0577	0.1202
R-507[A]	-12.54	0.1792	-0.00069	1.769×10^{-6}	-1.49×10^{-9}	1	0.0049	0.0350
R421B	-45.95	0.6093	-0.00267	5.61×10^{-6}	-4.20×10^{-9}	0.9974	0.3605	0.3002
R423A	70.69	-0.7661	0.003498	-6.78×10^{-6}	5.11×10^{-9}	0.9824	1.712	0.7555

mole fractions of corresponding components. AADs of the viscosities for R125-R134a and R125-R32 systems were estimated to be 0.754% and 1.005%, respectively.

Predicted thermal conductivities were also compared with the experimental ones. Figure 3 displays the deviations of calculated thermal conductivities for the two binary

Table 10. Predicted Transport Properties of the some Industrial Ternary Mixtures

	R404 A		R407 C		R407 E		R425A	
T	η	λ	η	λ	η	λ	η	λ
(K)	(μpa s)	(mW mK^{-1})	(μpa s)	(mW mK^{-1})	(μpa s)	(mW mK^{-1})	(μpa s)	(mW mK^{-1})
200	7.853	-	8.151	-	8.022	-	7.941	-
250	9.885	10.902	10.391	10.742	9.042	9.931	10.008	-
273.15	10.838	12.578	11.441	12.377	11.073	12.304	10.965	12.062
293.15	11.667	14.179	12.354	13.649	12.000	13.562	11.802	13.518
300	11.930	14.691	12.668	14.146	12.286	14.062	12.081	14.027
313.15	12.437	15.733	12.627	15.117	12.813	15.039	12.600	15.016
333.15	13.230	17.413	13.758	16.652	13.618	16.579	13.355	16.568
353.15	14.056	19.180	14.613	18.259	14.436	18.198	14.218	18.185
373.15	14.824	20.980	15.461	19.925	15.237	19.854	15.009	19.818
423.15	16.683	25.625	17.514	24.190	17.134	24.157	16.894	24.024
473.15	18.532	-	19.547	-	19.014	-	18.769	-
523.15	20.245	-	21.488	-	20.752	-	20.501	-
573.15	21.993	-	23.405	-	22.475	-	22.235	-
623.15	23.554	-	24.194	-	24.099	-	23.848	-
673.15	25.119	-	25.845	-	25.660	-	25.414	-
723.15	26.686	-	27.467	-	27.202	-	26.966	-
773.15	28.091	-	29.032	-	28.664	-	28.427	-
873.15	30.903	-	32.056	-	31.461	-	31.251	-
973.15	33.517	-	34.959	-	34.121	-	33.927	-

refrigerant mixtures, R507[A] and R410A, and the two ternary refrigerant mixtures, R407C and R404A, from the experimental data [42]. It should be mentioned that the thermal conductivities and heat capacities of the pure species, required by Schreiber et al.'s method [17], to calculate mixture thermal conductivities, were taken from the NIST data [34]. The AAD values of our calculated thermal conductivities for R507[A], R410A, R407C, and R404A mixtures from the experimental ones were found to be 9.173%, 7.489%, 7.987%, and 10.333%, respectively.

Close assessment of the obtained errors, while comparing the calculated viscosity values with the experimental data, reveals the dependency of the AAD values, to the mixture's composition. For example as we compare the AAD values for R410A and R507A binary mixtures, containing the R125 constituent in common,

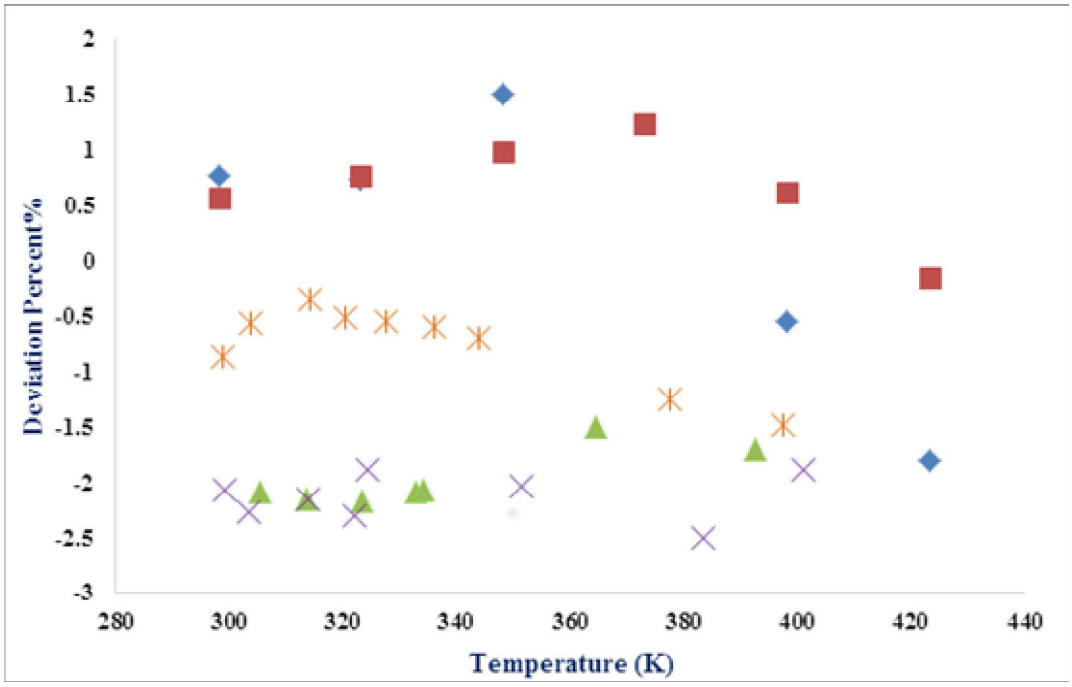

Fig. 1. Deviation plot for calculated viscosities of the three ternary and two binary refrigerant mixtures: R407C (♦), R404A (▲) and R407E (■), as the ternary mixtures [38,39], and R410A (✳) and R507[A] (×) as binary mixtures [38], compared with the experiment.

greater AAD value for R507A may be attributed to the presence of R143a component, instead of R32 which is present in the R410A mixture.

Even in the case of ternary mixtures, the R404A mixture having the R143a component, shows greater AAD value for the viscosity data compared to the other two ternary mixtures, lacking this component. It is interesting that both for the binary and ternary mixtures having R143a, greater AAD values for the thermal conductivity data is also observed.

On the other hand, comparing the AAD values for the viscosity data of binary and ternary mixtures, does not show any meaningful dependence on the number of mixture components.

Due to the importance of refrigerant mixtures in refrigeration engineering, and the limited data for the gaseous state, against liquid state in a wider range of pressures and temperatures, this section of the paper focuses on viscosity of several industrially binary mixtures of HFC-refrigerants at moderate pressures. The Eqs. (17)-(28), based on the Vesovic Wakeham's (VW) method [18], were used to predict the high-density viscosity values of the R421B and R410A mixtures. Numerical values of this property in a wider range of temperatures are presented in Tables 11 and 12.

The necessary densities of the aforementioned mixtures, required by the VW method, were obtained from the Peng Robinson equation of state [43]. Viscosity values of the pure components of these mixtures, required as input for the VW method, were extracted from the NIST database [34]. All calculations were conducted for temperature and pressure conditions in which the system exists in the gas phase. There were not any reported literature data on the moderate density viscosities of R410A and R421B mixtures, to be compared with our predicted viscosities. These two mixtures are composed of (R125-R134a) and (R125-R32) refrigerants. Fortunately there are some experimental data for other molar compositions of these binary mixtures. So, we calculated the deviation plots for

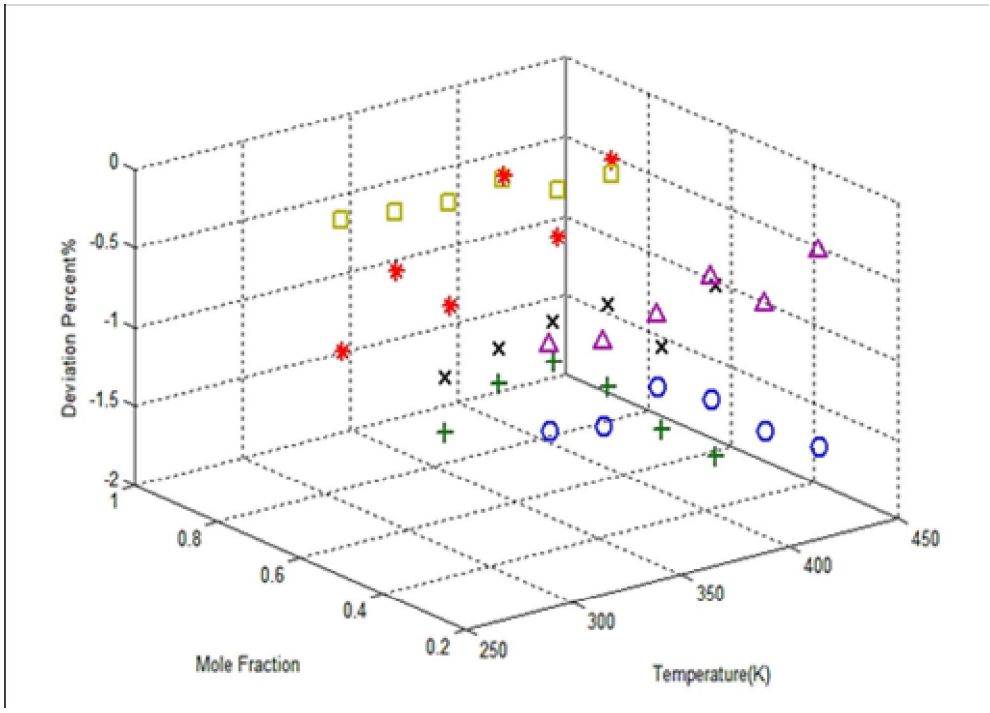

Fig. 2. Deviation plot for the calculated viscosity coefficients of the two binary refrigerant mixtures at different temperatures and mole fractions, compared with the experiment: (R125-R134a) [40] [x (R125) = 0.7510 (□), 0.5001 (×), and 0.2508 (Δ)], and (R125-R32) [41] [x (R125)= 0.2475 (○), 0.4998 (+), and 0.7498 (*)].

Table 11. The Predicted Dense Viscosities of R410A Binary Mixture

	η (μPa.s)				
T (K)	6 atm	8 atm	10 atm	12 atm	14 atm
300	12.7511	12.6630	12.5296	12.3202	11.9678
313.15	13.3662	13.3197	13.2400	13.1003	12.8188
	10 atm	15 atm	20 atm	25 atm	30 atm
333.15	14.3885	14.4961	14.6611	15.2055	15.6867
	20 atm	40 atm	60 atm	80 atm	100 atm
353.15	15.5860	17.9650	32.7676	47.5572	55.5837
373.15	16.3419	18.1142	22.4975	31.8708	37.7601
	20 atm	40 atm	60 atm	80 atm	90 atm
423.15	18.3996	19.1485	20.5746	22.0604	22.5511

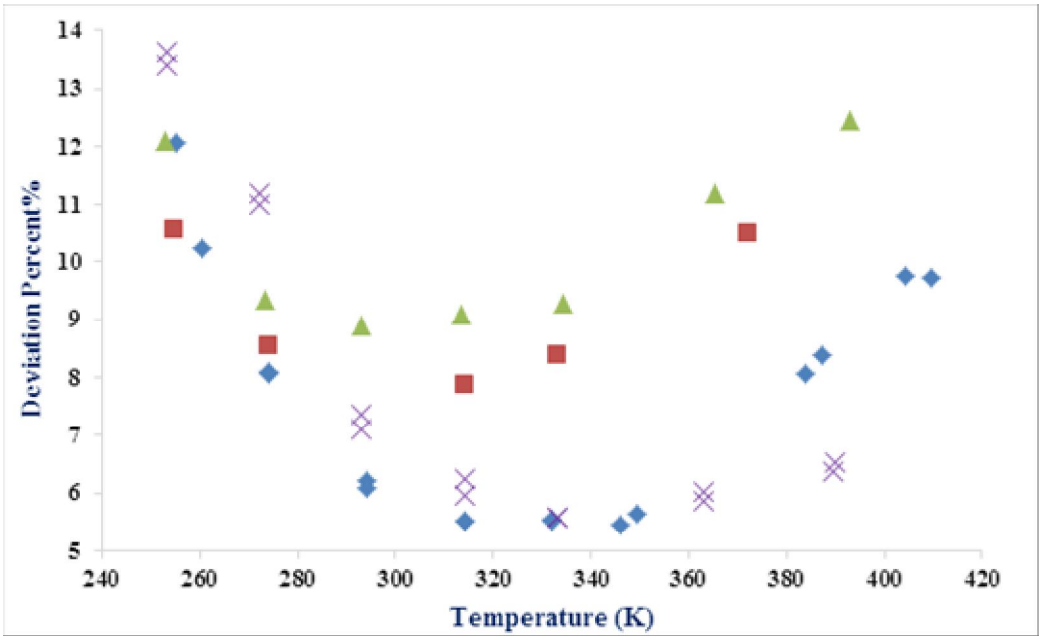

Fig. 3. Deviation plot for the calculated thermal conductivities of the two binary refrigerant mixtures, R507[A] (■) and R410A (♦), and the two ternary refrigerant mixtures, R407C (×) and R404A (▲) [42].

Table 12. The Predicted Dense Viscosities of R421B Binary Mixture

	η (μPa.s)				
T (K)	8 atm	10 atm	12 atm	14 atm	16 atm
333.15	14.3914	14.4711	14.5662	14.6775	14.8035
	7 atm	10 atm	15 atm	20 atm	25 atm
353.15	15.1531	15.2749	15.5552	15.9648	16.5770
	10 atm	15 atm	20 atm	25 atm	30 atm
373.15	16.0453	16.2965	16.6390	17.1033	17.7304
	20 atm	40 atm	60 atm	80 atm	100 atm
423.15	18.5857	20.3289	23.4153	27.2465	29.6297

predicted dense viscosities of (R125-R134a) and (R125-R32) mixtures, at different mole fractions of R125, compared with literature data [40,41]. Figures 4, 5 and 6 show the deviation plots for R125-R32 mixtures at temperatures 348.15 K, 373.15 K and 423.15 K, respectively. AAD (Absolute Average Deviation) values for

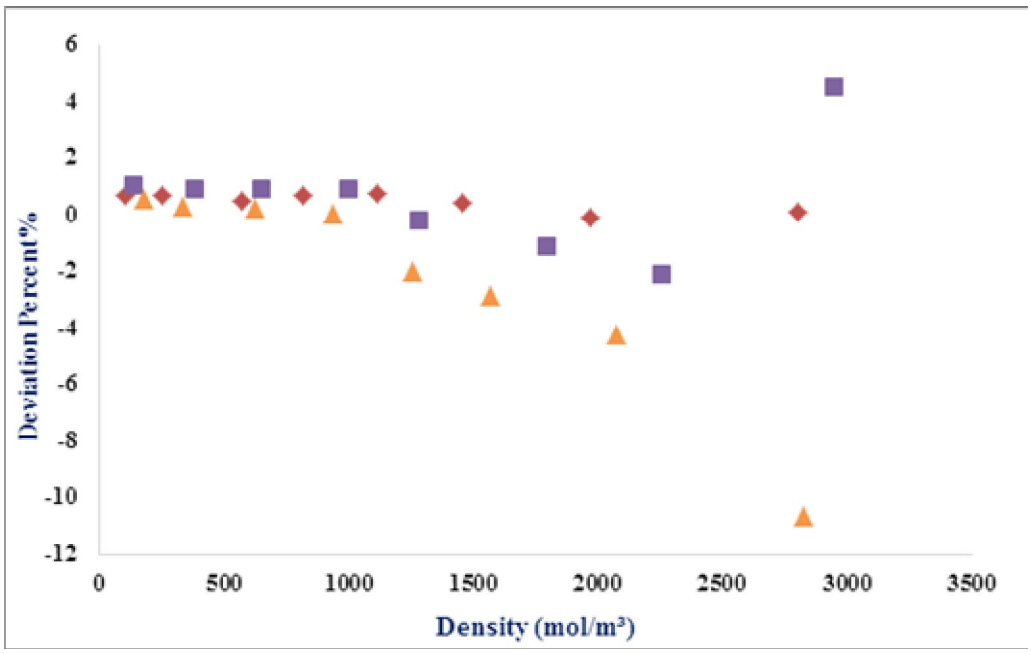

Fig. 4. Deviation plot for the viscosities of R125-R32 gaseous mixture in terms of density and different mole fractions of R125 at T = 348.15K: x_{R125} = 0.7498 (♦), x_{R125} = 0.4998 (■), x_{R125} = 0.2475 (▲) compared with the experimental data [41].

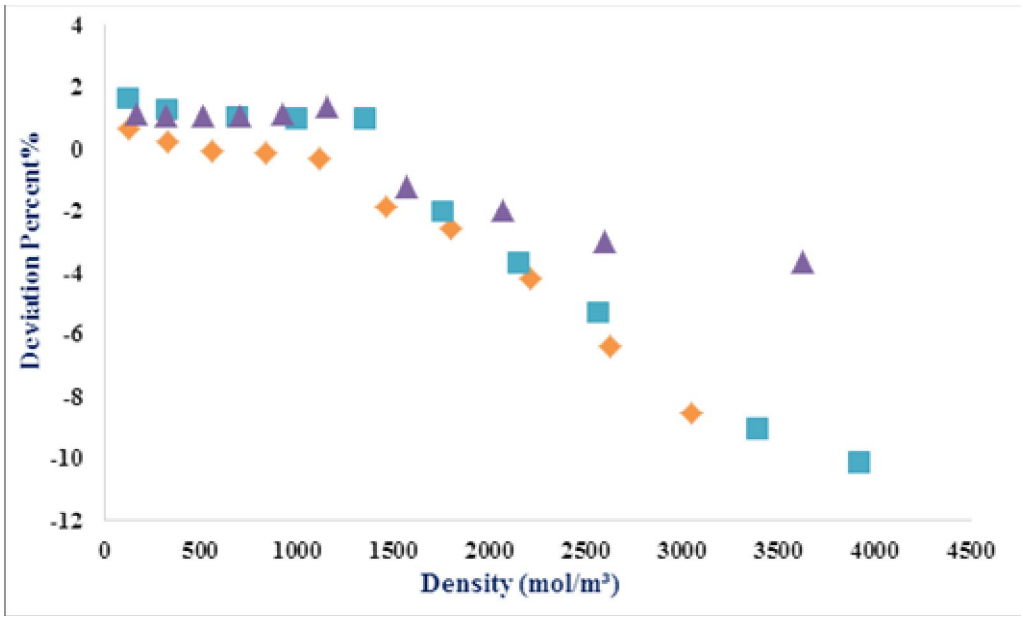

Fig. 5. Deviation plot for the viscosities of R125-R32 gaseous mixture in terms of density and different mole fractions of R125 at T = 373.15K: x_{R125} = 0.7498 (♦), x_{R125} = 0.4998 (■), x_{R125} = 0.2475 (▲) compared with the experimental data [41].

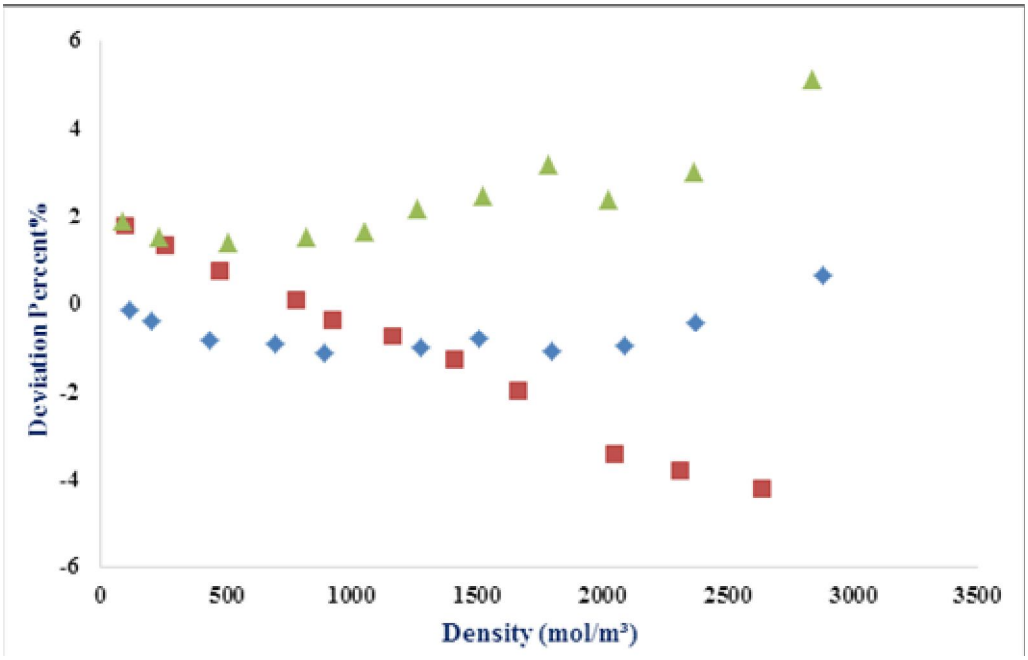

Fig. 6. Deviation plot for the viscosities of R125-R32 gaseous mixture in terms of density and different mole fractions of R125 at T = 423.15K: x_{R125} = 0.7498 (♦), x_{R125} = 0.4998 (■), x_{R125} = 0.2475 (▲), compared with the experimental data [41].

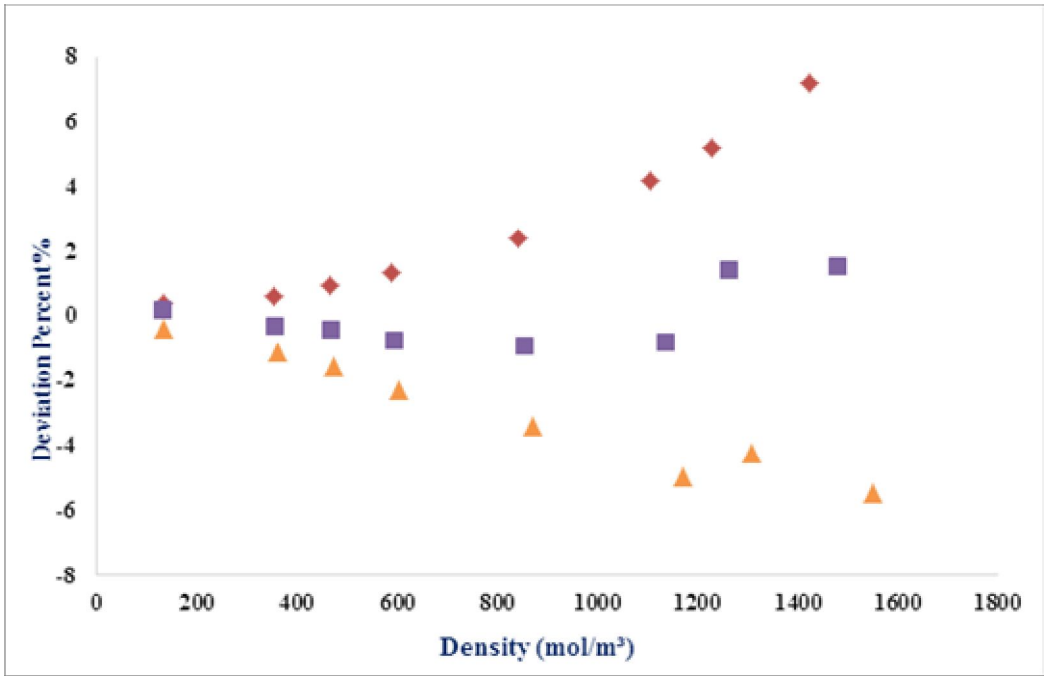

Fig. 7. Deviation plot for the viscosities of R125-134a gaseous mixture in terms of density and different mole fractions of R125 at T = 373.15K: x_{R125} = 0.7510 (♦), x_{R125} = 0.5001 (■), x_{R125} = 0.2508 (▲), compared with the experimental data [40].

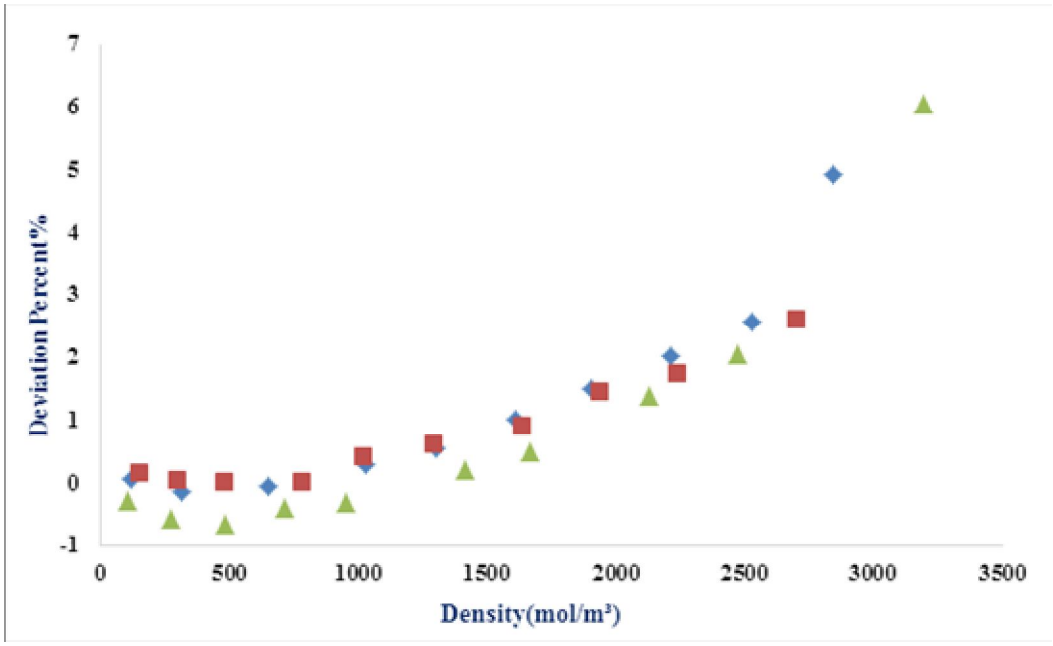

Fig. 8. Deviation plot for the viscosities of R125-R134a gaseous mixture in terms of density and different mole fractions of R125 at T = 398.15K: x_{R125} = 0.7510 (♦), x_{R125} = 0.5001 (■), x_{R125} = 0.2508 (▲), compared with the experimental data [40].

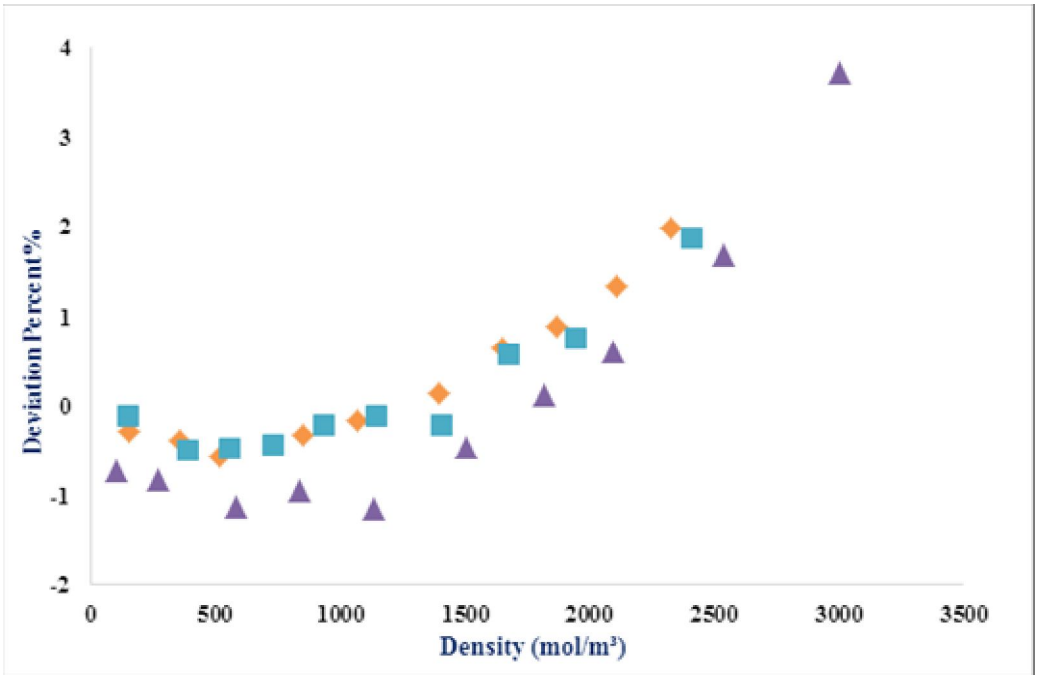

Fig. 9. Deviation plot for the viscosities of R125-R134a gaseous mixture in terms of density and different mole fractions of R125 at T = 423.15K: x_{R125} = 0.7510 (♦), x_{R125} = 0.5001 (■), x_{R125} = 0.2508 (▲), compared with the experimental data [40].

this mixture at temperatures 348.15 K, 373.15 K and 423.15 K were found to be 1.52%, 2.59%, and 1.65% respectively [41].

In addition, Figs. 7, 8 and 9 are deviation plots for the viscosity coefficients of R125-R134a binary mixtures at temperatures 373.15 K, 398.15 K and 423.15 K, where the respective AAD values were computed to be equal to 1.31%, 2.18%, and 0.78% [40]. In the case of R410A binary mixture, the high density viscosity values show decrease with the pressure at temperatures 300 K and 313.15 K. This behavior, which is opposite to the expected trend, has also been observed in previous literature values [41]. Nabizadeh and Mayinger have reported this kind of observation for some refrigerants. They mention that at highly superheated and supercritical temperatures, viscosity increases with increasing pressure (density), whereas at subcritical temperatures the viscosity of halogenated hydrocarbons reveals a strange behavior in which the viscosity decreases with increasing pressure [44]. Note that the critical point for R410A is 72.8 °C (348.15 K).

CONCLUSIONS

After determination of inverted potential energies for some industrial HFC refrigerants, the Chapman-Enskog and Vesovic-Wakeham methods were employed respectively to calculate the transport properties of binary and ternary refrigerant mixtures, at low and moderate density regimes. Successful agreement between our obtained results with the available literature data confirms the applicability of the inversion method in acceptable determination of refrigerant potential energies and corresponding collision integrals, necessary to calculate transport properties through the Chapman-Enskog and the Vesovic-Wakeham methods.

ACKNOWLEDGEMENTS

The authors would like to thank Shiraz University of Technology for supporting this project.

REFERENCES

[1] He, M.; Qi, X.; Liu, X.; Su, C.; Lv, N. J. I. J. o. R., Estimating the viscosity of pure refrigerants and their mixtures by free-volume theory. *Int. J. Refrig.* **2015**, *54*, 55-66.DOI: 10.1016/j.ijrefrig.2015.03.010.

[2] Alavianmehr, M. M.; Behnejad, H.; Jahangiri, S.; Hosseini, S. M. J. P., Thermodynamic properties of refrigerants from SM sound velocity-based equation of state. *Phys. Chem. Liq.* **2014**, *52*, 546-555. DOI: 10.1080/00319104.2013.852477.

[3] Mohanraj, M.; Muraleedharan, C.; Jayaraj, S. J. I. j. o. e. r., A review on recent developments in new refrigerant mixtures for vapour compression-based refrigeration, air-conditioning and heat pump units. *Int. J. Energy Res.* **2011**, *35*, 647-669. DOI: 10.2514/6.2003-3915.

[4] Avsec, J.; Oblak, M. In The analytical calculation of thermal conductivity, viscosity and thermal diffusivity for binary and ternary mixtures, 36th AIAA Thermophysics Conference, 2003, p. 3915.

[5] Gao, X.; Assael, M.; Nagasaka, Y.; Nagashima, A., Prediction of the thermal conductivity and viscosity of binary and ternary HFC refrigerant mixtures. *Int. J. Thermophys.* **2000**, *21*, 23-34. DOI: 10.1023/A:1006696518938.

[6] Goharshadi, E. K.; JamiAlahmadi, M.; Najafi, B. J. C. J. O. C., Determination of potential energy functions of argon, krypton, and xenon *via* the inversion of reduced-viscosity collision integrals at zero pressure. *Can. J. Chem.* **2003**, *81*, 866-871. DOI: 10.1139/v03-095.

[7] Clancy, P.; Gough, D.; Matthews, G.; Smith, E.; Maitland, G., Simplified methods for the inversion of thermophysical data. *Mol. Phys.* **1975**, *30*, 1397-1407. DOI: 10.1080/00268977500102921.

[8] Barker, J.; Watts, R.; Lee, J. K.; Schafer, T.; Lee, Y. -T., Interatomic potentials for krypton and xenon. *J. Chem. Phys.* **1974**, *61*, 3081-3089. DOI: 10.1063/1.1682464.

[9] Maitland, G.; Smith, E. J. M. P., The intermolecular pair potential of argon. *Mol. Phys.* **1971**, *22*, 861-868. DOI: 10.1080/00268977100103181.

[10] Gough, D.; Smith, E.; Maitland, G. J. M. P., The pair potential energy function for krypton. *Mol. Phys.* **1974**, *27*, 867-872. DOI: 10.1080/00268977400100781.

[11] Haghighi, B.; Fathabadi, M.; Papari, M. J. F. p. e.,

Calculation of the transport properties of CO-noble gases mixtures at low density by the semi-empirical inversion method. *Fluid Phase Equilib.* **2002**, *203*, 205-225. DOI: 10.1016/S0378-3812(02)00191-7.

[12] Mohammad-Aghaie, D.; Papari, M. M.; Zargari, F. J. B. o. t. C. S. o. J., Modeling transport properties of N2-noble gas mixtures at low and moderate densities. *Bull. Chem. Soc. Japan* **2012**, *85*, 563-575. DOI: 10.1246/bcsj.20110329.

[13] Zargari, F.; Mohammad-Aghaie, D.; Lotfi, M.; Ghorbanipour, M.; Alavianmehr, M. M.; Shahraki, O. J. C. j. o. c. e., Transport properties of dilute ammonia-noble gas mixtures from new intermolecular potential energy functions. *Chin. J. Chem. Eng.* **2017**, *25*, 1727-1734.

[14] Mohammad-Aghaie, D.; Papari, M. M.; Ebrahimi, A. R. J. C. J. o. C. E., Determination of transport properties of dilute binary mixtures containing carbon dioxide through isotropic pair potential energies. *Chin. J. Chem. Eng.* **2014**, *22*, 274-286. DOI: 10.1016/S1004-9541(14)60018-5.

[15] Moghadasi, J.; Mohammad-Aghaie, D.; Papari, M. J. I.; research, e. c., Predicting gas transport coefficients of alternative refrigerant mixtures. *Ind. Eng. Chem. Res.* **2006**, *45*, 9211-9223. DOI: 10.1021/ie060630v.

[16] Chapman, S.; Cowling, T. G.; Burnett, D., The mathematical theory of non-uniform gases: an account of the kinetic theory of viscosity, thermal conduction and diffusion in gases. Cambridge university press: 1990.

[17] Schreiber, M.; Vesovic, V.; Wakeham, W. J. I. j. o. t., Thermal conductivity of multicomponent polyatomic dilute gas mixtures. *Int. J. Thermophys.* **1997**, *18*, 925-938. DOI: 10.1007/BF02575238.

[18] Vesovic, V.; Wakeham, W. J. C. E. S., Prediction of the viscosity of fluid mixtures over wide ranges of temperature and pressure. *Chem. Eng. Sci.* **1989**, *44*, 2181-2189. DOI: 10.1016/0009-2509(89)85152-8.

[19] Vesovic, V.; Wakeham, W. J. I. J. o. T., The prediction of the viscosity of dense gas mixtures. *Int. J. Thermophys.* 1989, *10*, 125-132.DOI: 10.1007/ BF00500713.

[20] Enskog, D., Kinetische Theorie der Vorgänge in mässig verdünnten Gasen, 1917.

[21] Hirschfelder, J.; Bird, R. B.; Curtiss, C. F., Molecular theory of gases and liquids. **1964**. DOI: http://cds.cern.ch/record/108119.

[22] Thijsse, B.; Hooft, G. t.; Coombe, D.; Knaap, H.; Beenakker, J. J. P. A. S. M.; Applications, i., Some simplified expressions for the thermal conductivity in an external field. *Phys. A (Amsterdam, Neth.)* **1979**, *98*, 307-312.DOI: 10.1016/0378-4371(79)90181-X.

[23] Di Pippo, R.; Dorfman, J.; Kestin, J.; Khalifa, H.; Mason, E., Composition dependence of the viscosity of dense gas mixtures. *Phys. A (Amsterdam, Neth.) and its Applications* **1977**, *86*, 205-223.DOI: 10.1016/0378-4371(77)90029-2.

[24] Di Pippo, R.; Dorfman, J.; Kestin, J.; Khalifa, H.; Mason, E., Composition dependence of the viscosity of dense gas mixtures. *Phys. A (Amsterdam, Neth.) its Applications* **1977**, *86*, 205-223.DOI: 10.1016/0378-4371(77)90029-2.

[25] Sandler, S. I.; Fiszdon, J. K. J. P. A. S. M.; Applications, i., On the viscosity and thermal conductivity of dense gases. *Phys. A (Amsterdam, Neth.)* **1979**, *95*, 602-608. DOI: 10.1016/0378-4371(79)90036-0.

[26] Millat, J.; Dymond, J.; de Castro, C. N.; Wakeham, W., Transport properties of fluids. Cambridge University Press Cambridge, 1996.

[27] Kestin, J.; Wakeham, W. J. B. d. B. f. p. C., Calculation of the influence of density on the thermal conductivity of gaseous mixtures. *Berichte der Bunsengesellschaft für Physikalische Chemie* **1980**, *84*, 762-769. DOI: 10.1002/bbpc.19800840815.

[28] Bzowski, J.; Kestin, J.; Mason, E.; Uribe, F., Equilibrium and transport properties of gas mixtures at low density: Eleven polyatomic gases and five noble gases. *J. Phys. Chem. Ref. Data* **1990**, *19*, 1179-1232. DOI: 10.1063/1.555867.

[29] Gatland, I.; Viehland, L.; Mason, E. J. P. A. S. M., Tests of alkali ion-inert gas interaction potentials by gaseous ion mobility experiments. *J. Chem. Phys.* **1977**, *66*, 537-541. DOI: 10.1063/1.433973.

[30] O'Hara, H.; Smith, F. J. J. J. o. c. p., The efficient calculation of the transport properties of a dilute gas to a prescribed accuracy. *J. Comput. Phys.* **1970**, *5*, 328-344. DOI: 10.1016/0021-9991(70)90065-3.

[31] O'Hara, H.; Smith, F. J., Transport collision integrals for a dilute gas. *Comput. Phys. Commun.* **1971**, *2*, 47-54. DOI: 10.1016/S0010-4655(84)82329-2.

[32] Tosi, M.; Fumi, F. J. J. o. P.; Solids, C. o., Ionic sizes and born repulsive parameters in the NaCl-type alkali halides-II: The generalized Huggins-Mayer form. *J. Phys.* **1964**, *25*, 45-52. DOI: 10.1016/0022-3697(64)90160-X.

[33] Fumi, F. G.; Tosi, M., Ionic sizes and born repulsive parameters in the NaCl-type alkali halides-I: The Huggins-Mayer and Pauling forms. *J. Phys. Chem. Solids* **1964**, *25*, 31-43. DOI: 10.1016/0022-3697(64)90159-3.

[34] Lemmon, E. J. N. C. W., Thermophysical properties of fluid systems, 2003.

[35] Nabizadeh, H.; Mayinger, F. J. H. T. H. P., Viscosity of gaseous R123, R134a, and R142b. High Temp-*High Press.* **1992**, *24*, 221-230.

[36] Chung, T. H.; Ajlan, M.; Lee, L. L.; Starling, K. E., Generalized multiparameter correlation for nonpolar and polar fluid transport properties. *Ind. Eng. Chem. Res.* **1988**, *27*, 671-679. DOI: 10.1021/ie00076a024.

[37] Maitland, G.; Rigby, M.; Smith, E.; Wakeham, W.; Henderson, D. J. P. T., Intermolecular forces: their origin and determination. *Phys. Today* **1983**, *36*, 57.

[38] Nabizadeh, H.; Mayinger, F. J. I. j. o. t., Viscosity of Gaseous R404A, R407C, R410A, and R507. *Int. J. Thermophys.* **1999**, *20*, 777-790. DOI: 10.1023/A:1022618832289.

[39] Yokoyama, C.; Takahashi, M.; Tomida, D. J. I. j. o. t., Viscosity of Alternative Refrigerants R407C and R407E in the Vapor Phase from 298.15 to 423.15 K. *Int. J. Thermophys.* **2006**, *27*, 699-713. DOI: 0.1007/s10765-006-0052-3.

[40] Yokoyama, C.; Nishino, T.; Takahashi, M. J. F. p. e., Viscosity of gaseous mixtures of HFC-125 (pentafluoroethane) + HFC-134a (1,1,1,2-tetrafluoroethane) under pressure. *Fluid Phase Equilib.* **2000**, *174*, 231-240. DOI: 10.1016/S0378-3812(00)00430-1.

[41] Yokoyama, C.; Nishino, T.; Takahashi, M. J. I. j. o. t., Viscosity of gaseous mixtures of HFC-125 + HFC-32. *Int. J. Thermophys.* **2001**, *22*, 1329-1347. DOI: 10.1023/A:1012882017926.

[42] Geller, V.; Nemzer, B.; Cheremnykh, U. J. I. j. o. t., Thermal conductivity of the refrigerant mixtures R404A, R407C, R410A, and R507A. *Int. J. Thermophys.* **2001**, *22*, 1035-1043. DOI: 10.1023/A:1010691504352.

[43] Peng, D. -Y.; Robinson, D. B., A new two-constant equation of state. *Industrial & Engin. Chem. Fundamentals* **1976**, *15*, 59-64. DOI: 10.1021/i160057a011.

[44] Nabizadeh, H.; Mayinger, F. J. I. j. o. t., Viscosity of refrigerants R12, R113, and R114 and mixtures of R12 + R114 at high pressure. *Int. J. Thermophys.* **1989**, *10*, 701-712. DOI: 10.1007/BF00507990.